

1 **Mixed-Phase Cloud Feedbacks**

2 Daniel T. McCoy, Dennis L. Hartmann, Mark D. Zelinka

3 **Abstract**

4 This chapter introduces cloud feedbacks and describes salient features of their structure.

5 One particularly pronounced feature simulated by global climate models (GCMs), is the
6 contrast between the subtropics where cloud cover decreases with warming (a positive
7 feedback) and the mid- and high-latitudes where cloud albedo increases with warming (a
8 negative feedback). This increase in cloud albedo appears to be due to mixed-phase
9 clouds (MPCs) transitioning from a more ice-dominated to more liquid-dominated state.

10 The representation of this behavior in GCMs is discussed and is compared to satellite
11 observations. Observational constraints on the mixed-phase cloud feedback show that the
12 current generation of GCMs have too strong an increase in planetary albedo due to ice
13 transitioning to liquid in the mid- and high-latitudes, indicating a potential
14 underestimation of climate sensitivity. This behavior appears to be at least partially due to
15 an inability to maintain supercooled liquid water at sufficiently low temperatures.

16 **Keywords: Cloud feedback, global climate models, climate sensitivity, satellite**
17 **observations, model tuning, Southern Ocean, emergent constraints**

19 **Introduction**

20 Oceanic planetary boundary layer (PBL) cloud cover strongly affects reflected
21 shortwave (SW) radiation, but has relatively little effect on the outgoing longwave (LW).
22 This leads to a negative cloud radiative effect (CRE) that strongly affects the Earth's
23 radiative balance [*Hartmann and Short, 1980*]. Because of this it is important to represent
24 the response of PBL cloud to warming accurately to calculate 21st century climate
25 change. Unfortunately, PBL clouds must be parameterized in GCMs. This is because
26 turbulent motions with length scales smaller than a GCM grid cell create boundary-layer
27 cloud. The ability of the PBL cloud parameterizations to reproduce cloud behavior in the
28 current climate can be evaluated using observations, however it is difficult to use the

29 existing observational record to evaluate the accuracy of the response of PBL cloud to
30 warming. This results in a cloud feedback that is highly uncertain, even in the most recent
31 generation of GCMs [*Bony et al.*, 2006; *Caldwell et al.*, 2013; *Vial et al.*, 2013; *Webb et*
32 *al.*, 2013] and accounts for most of the uncertainty in the estimation of equilibrium
33 climate sensitivity (ECS) [*Vial et al.*, 2013; *Webb et al.*, 2006].

34 Even though the global cloud feedback varies widely across GCMs the spatial
35 structure of GCM cloud feedbacks are relatively similar [*Zelinka et al.*, 2012; *Zelinka et*
36 *al.*, 2016; *Zelinka et al.*, 2013]. One particularly striking feature is the similarity in the
37 latitudinal pattern of the response of cloud SW reflection to warming. We will refer to
38 this change in the reflection of SW due to changes in cloud optical depth and amount
39 with warming as the SW cloud feedback. The SW cloud feedback over oceans in the fifth
40 climate model intercomparison project (CMIP5) is shown in Figure 1. Across GCMs the
41 SW cloud feedback transitions from positive in the subtropics to negative poleward of
42 around 50°. This is particularly pronounced in the Southern Hemisphere, but also occurs
43 in the Northern Hemisphere. In GCMs this effect is not strongly coupled to shifts in
44 midlatitude jet position [*Bender et al.*, 2011; *Ceppi and Hartmann*, 2015; *Ceppi et al.*,
45 2014; *Grise and Medeiros*, 2016]. The SW cloud feedback may be decomposed into
46 contributions from cloud optical depth, amount, and altitude [*Zelinka et al.*, 2012]. The
47 contributions from amount and optical depth, which dominate the SW, are shown in
48 Figure 1. It is clear that the majority of the positive subtropical feedback originates from
49 cloud area decreasing and revealing the relatively dark ocean beneath, while the negative
50 midlatitude feedback is due to increasing cloud optical depth.

51 << Insert Figure 1 here >>

52 Decreasing cloud cover with warming has been studied extensively and is a robust
53 feature of both large eddy simulation and observational analysis [*Blossey et al.*, 2013;
54 *Bretherton*, 2015; *Bretherton and Blossey*, 2014; *Bretherton et al.*, 2013; *Clement et al.*,
55 2009; *Klein et al.*, 1995; *Myers and Norris*, 2013; 2015; 2016; *Norris and Leovy*, 1994;
56 *Norris et al.*, 2016; *Qu et al.*, 2014a; b; *Qu et al.*, 2015; *Rieck et al.*, 2012; *Seethala et al.*,
57 2015]. It is well known that increasing boundary layer stability increases cloud cover and
58 that boundary layer stability increases as the planet warms [*Klein and Hartmann*, 1993;
59 *Myers and Norris*, 2015; *Qu et al.*, 2014b; *Webb et al.*, 2013; *Wood and Bretherton*,

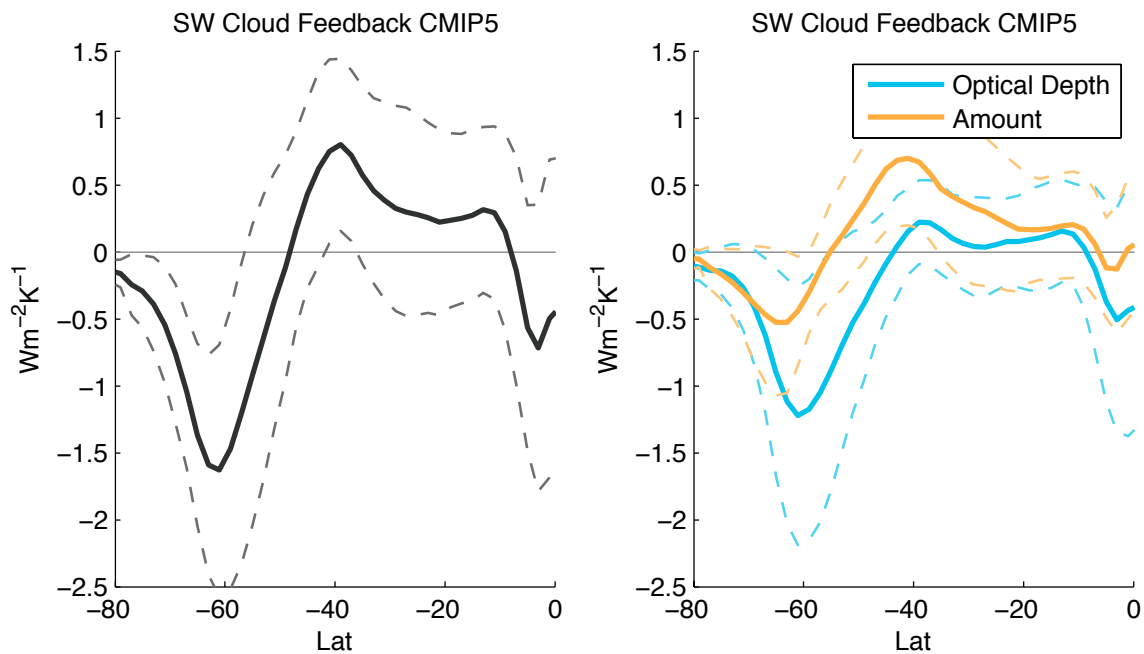
60 2006]. However, the increase in cloud cover due to increasing stability seems to be
61 overwhelmed by decreases driven by thermodynamic mechanisms linked to sea surface
62 temperature increases [Bretherton and Blossey, 2014]. This positive subtropical cloud
63 amount feedback increases equilibrium climate sensitivity (ECS), and the negative
64 feedback at high latitudes has a counterbalancing effect on ECS. The robustness of the
65 positive cloud amount feedback in the subtropics makes it particularly important to
66 understand whether the negative feedback in the mid-latitudes is physical, and if so, if its
67 strength is accurately represented.

68 The potential for a pronounced change in cloud optical depth due to mixed-phase
69 clouds transitioning to a relatively more liquid-dominated state was first noted by
70 Mitchell *et al.* [1989] and Li and Le Treut [1992]. Over the last decade this so-called
71 mixed-phase cloud feedback has been of increasing interest in the climate modeling
72 community [Ceppi *et al.*, 2016a; Choi *et al.*, 2014; Kay *et al.*, 2016; McCoy *et al.*, 2016;
73 Naud *et al.*, 2006; Tan and Storelvmo, 2016; Tan *et al.*, 2016; Tsushima *et al.*, 2006] and
74 has been recently featured in review articles [Gettelman and Sherwood, 2016; Storelvmo
75 *et al.*, 2015]. It appears that representing mixed-phase cloud behavior in a way that is
76 both physically robust and tractable from a modeling standpoint is becoming a widely
77 acknowledged challenge in accurately predicting 21st century climate change.

78 As discussed in Mitchell *et al.* [1989] and Li and Le Treut [1992], the increase in
79 cloud optical depth in the mid-latitudes appears to be due to transitions of mixed-phase
80 cloud cover to a relatively less ice-dominated and more liquid-dominated state. At zero-th
81 order this is simply because ice crystals tend to be larger than liquid droplets and thus less
82 reflective for a constant amount of condensate [McCoy *et al.*, 2014; Tsushima *et al.*,
83 2006; Zelinka *et al.*, 2012]. In addition to this effect it is probable that the cloud water
84 mass will increase with warming because ice precipitates much more efficiently than
85 liquid [Ceppi *et al.*, 2016a; Field and Heymsfield, 2015; Heymsfield *et al.*, 2009; McCoy
86 *et al.*, 2015a; Mitchell *et al.*, 1989; Morrison *et al.*, 2011]. This *mixed-phase cloud*
87 *feedback* is the subject of this chapter.

88 The mixed-phase cloud feedback is particularly difficult to constrain in GCMs for
89 several reasons. These may be generally grouped into bottom-up and top-down
90 uncertainties. From the bottom-up, the mixed-phase cloud feedback is uncertain because

91 it is governed by ice nucleation; and other mixed-phase cloud physics, which are a
 92 complex interplay of different mechanisms, many of which still lack a strong constraint
 93 [Atkinson *et al.*, 2013; Hoose and Möhler, 2012; H Morrison *et al.*, 2011; Murray *et al.*,
 94 2012; Tan and Storelvmo, 2016]. From the top down the feedback is uncertain because
 95 we cannot accurately measure the amount of cloud ice mass, making it difficult for
 96 models to be rigorously evaluated [Carro-Calvo *et al.*, 2016; Hu *et al.*, 2010; Jiang *et al.*,
 97 2012]. Together, these top-down and bottom-up uncertainties yield a wide variety of
 98 mixed-phase behaviors in climate models and have led to mixed-phase cloud feedbacks
 99 being one of the major contributors to uncertainty in the cloud feedback, and thus climate
 100 sensitivity [McCoy *et al.*, 2016; Zelinka *et al.*, 2016]. In this chapter we will discuss the
 101 origins, mechanisms, and possible constraints on this feedback.



102
 103 **Figure 1** The SW cloud feedback of GCMs participating in CMIP5. The figure on the left shows the multi-
 104 model mean SW cloud feedback with one standard deviation across the GCMs shown as a dashed line.
 105 The same figure is shown on the right, but with SW cloud feedback decomposed into contributions from
 106 optical depth and amount feedbacks (see Zelinka *et al.* [2012]).

107

108 **The Mixed-Phase Cloud Feedback in GCMs**

109 As we discussed in the introduction, understanding the robustness and strength of
 110 the mixed-phase cloud feedback in GCMs is important for better constraining ECS and

111 offering better predictions of 21st century climate change [*Tan et al.*, 2016]. Because
112 mixed-phase cloud physics operate at a length scale smaller than global climate model
113 resolution their behavior in GCMs must be parameterized. Readers interested in a more
114 in-depth discussion of how MPCs are parameterized in GCMs should read chapter <<cite
115 Kali Furtado's chapter on mixed-phase cloud parameterization>> of this text.

116 As noted above, parameterization of mixed-phase cloud physics is not the focus
117 of this chapter, but it is useful to discuss it briefly. When confronted with the need to
118 represent mixed-phase clouds, GCMs may either attempt to represent the nucleation of
119 ice by aerosol and the growth of ice particles in MPCs, or may simply diagnose the
120 partitioning of ice and liquid based on a function of temperature [*Cesana et al.*, 2015;
121 *Tsushima et al.*, 2006]. Both approaches are problematic. Diagnosing liquid fraction as a
122 function of atmospheric temperature is a very stable method of describing mixed-phase
123 clouds, and can be implemented based on aircraft sampling of clouds (see *Bower et al.*
124 [1996]), however it cannot represent the impacts of regional variability in ice nuclei (IN)
125 on supercooled liquid clouds [*Atkinson et al.*, 2013; *Kanitz et al.*, 2011; *Murray et al.*,
126 2012]. Indeed, when observed over large regions, differences in cloud cover in regions
127 that have access to IN (particularly dust) have noticeably less supercooled liquid [*Hu et*
128 *al.*, 2010; *Kanitz et al.*, 2011; *Tan et al.*, 2014]. Sources of IN, particularly feldspar, are
129 much more common in the Northern Hemisphere than in the Southern Hemisphere,
130 leading to Northern Hemisphere clouds being more glaciated [*Atkinson et al.*, 2013; *A E*
131 *Morrison et al.*, 2010; *Murray et al.*, 2012].

132 While mixed-phase cloud processes are complex, when a mixed-phase cloud is
133 warmed it should transition from a more ice-dominated to a more liquid-dominated state
134 as sinks of cloud water through ice-phase precipitation are suppressed [*Ceppi et al.*,
135 2016a; *McCoy et al.*, 2015a; *Mitchell et al.*, 1989; *H Morrison et al.*, 2011]. Because of
136 the difference in the radiative properties of ice and liquid this results in an increase in
137 upwelling SW and a negative optical depth feedback, providing that the size of ice
138 crystals and liquid droplets are reasonably represented in a given GCM.

139 Do GCMs all agree on the mixed-phase cloud temperature range? By examining
140 the behavior of mixed-phase clouds in GCMs as a function of atmospheric temperature it
141 becomes clear that climate models disagree strongly as to the temperature range inhabited

142 by mixed phase clouds. This is shown in Figure 2 for GCMs participating in CMIP5. To
143 create the curves shown in Figure 2 for each GCM the fraction of liquid condensate is
144 calculated within each model-level and latitude-longitude grid box. The fraction of liquid
145 condensate is then averaged as a function of atmospheric temperature. This yields a gross
146 statistical representation of the partitioning of ice and liquid as a function of temperature
147 within each model. Examination of these curves reveals substantial disagreement
148 between GCMs in terms of their mixed-phase condensate partitioning behavior. Some
149 GCMs maintain liquid water to temperatures as low as 220K, well below the
150 homogeneous freezing temperature, while some models are entirely composed of ice at
151 temperatures as high as 260K. Overall, there is a nearly 35K range across models where
152 ice and liquid are equally prevalent. While it is useful to discuss the temperature range
153 for which mixed-phase clouds exist in a particular GCM, we will utilize the temperature
154 at which ice and liquid are equally mixed for the remainder of this chapter. This is useful
155 for brevity and characterizing the mixed-phase cloud temperature range of each model by
156 a single number still has the capability to explain a significant amount of inter-model
157 variability. We will refer to this quantity, the atmospheric temperature at which ice and
158 liquid each make up 50% of existing condensate, as T5050 [McCoy *et al.*, 2016; Naud *et*
159 *al.*, 2006].

160 << Insert Figure 2 here >>

161 We have shown that in the models participating in CMIP5 there is an
162 approximately 35K range in the temperature where ice and liquid are equally prevalent
163 (Figure 2). Can the range of GCM ice to liquid partitioning shown in Figure 2 be
164 constrained using observations? As noted above, the curves in Figure 2 show the
165 temperature dependent partitioning of ice and liquid for vertical averages over GCM
166 model levels (see McCoy *et al.* [2015a] for calculation details). Because of this it is hard
167 to evaluate this model behavior with observations. Evidently this is not directly
168 comparable to in-situ measurements made from an airplane, because airplane
169 measurements are made in specific cloud regimes and at high temporal and spatial
170 resolutions [Bower *et al.*, 1996; Cober *et al.*, 2001; Isaac and Schemenauer, 1979;
171 Korolev and Isaac, 2003; Moss and Johnson, 1994; Mossop *et al.*, 1970; Storelvmo *et al.*,
172 2015].

173 A more direct comparison may be made between GCM phase partitioning and
174 ground- and space-based remote sensing. *Naud et al.* [2006] utilized Moderate Resolution
175 Imaging Spectroradiometer (MODIS) [*King et al.*, 2003] measurements of cloud top
176 phase in northern hemisphere cyclones to show that cloud tops were equally partitioned
177 between ice and liquid at roughly 255K in the Northern Hemisphere. Surface-based lidar
178 estimates made by *Kanitz et al.* [2011] showed a T5050 that varied between 242K for
179 pristine maritime regions and 260K for a continental site in Leipzig, Germany. This
180 contrast between pristine maritime regions away from dust sources and continental sites
181 is echoed by studies conducted using space-based lidar [*Hu et al.*, 2010; *Tan et al.*, 2014].
182 *Komurcu et al.* [2014] evaluated a selection of state of the art GCMs that do not treat ice
183 and liquid partitioning as a function of temperature alone. The simulated cloud lidar
184 output from these models showed that all six GCMs produced clouds that were much
185 more glaciated than observed by the CALIPSO lidar [*Winker et al.*, 2009]. This result is
186 reinforced by the analysis performed by *Cesana et al.* [2015] and *McCoy et al.* [2015a]
187 who diagnosed the effective ice to liquid partitioning curve used by several of the models
188 participating in CMIP5 (Figure 2). However, it was shown by *Cesana et al.* [2015] using
189 simulated lidar output from GCMs that lidar-diagnosed ice to liquid partitioning is not
190 directly comparable to the curves shown in Figure 2. This makes using space-borne
191 observations to constrain ice in mixed-phase clouds in models problematic. *McCoy et al.*
192 [2016] offered a rough estimate of the range where ice and liquid are equally mixed
193 based on results from *Cesana et al.* [2015] and *Hu et al.* [2010]. This range was estimated
194 at 254K-258K, in the global mean. This is a much smaller range than the range of
195 temperatures from CMIP5 models (shown as a shaded area in Figure 2), and supports the
196 idea that the current generation of GCMs tends to freeze liquid at temperatures that are
197 too high [*Cesana et al.*, 2015; *Komurcu et al.*, 2014; *McCoy et al.*, 2016].

198 The most apparent effect of this diversity in model parameterization manifests
199 itself in a wide variety of climatological cloud properties in GCMs. GCMs that maintain
200 liquid down to colder temperatures tend to both have more liquid and less ice, as one
201 would naïvely expect. This is shown in Figure 3 by examining how the T5050
202 temperature relates to the inter-model spread in historical LWP and IWP in CMIP5
203 GCMs. In addition, GCMs with a higher T5050 appear to have less overall cloud water

204 (ice and liquid combined), which is generally consistent with the idea of enhanced
205 precipitation efficiency in more glaciated clouds (see *H Morrison et al.* [2011], *Ceppi et*
206 *al.* [2016a], and *McCoy et al.* [2015a]).

207 <<Insert Figure 3 here>>

208 Mixed-phase parameterizations have the capability to substantially influence the
209 climate mean-state ice and liquid content in the mixed-phase regions. This variety in
210 GCM climate mean-state ice and liquid water content may potentially be due to the weak
211 observational constraint on ice-phase condensate in the current climate [*Jiang et al.*,
212 2012]. Only the MODIS and Cloudsat instruments offer estimates of the cloud ice water
213 content through the vertical extent of the atmosphere. MODIS only retrieves IWP while
214 the sun is up, which excludes nighttime and high-latitude winter. It is difficult to estimate
215 an error in this retrieval beyond errors engendered by the assumed particle size
216 distribution used in the retrieval and intercomparison of GCMs and observations by *Jiang*
217 *et al.* [2012] assigned a factor of two uncertainty in the IWP retrieval from MODIS. The
218 Cloudsat radar is highly sensitive to the partitioning of cloud ice and precipitation
219 [*Eliasson et al.*, 2011] as well as to the assumed particle size distribution [*Jiang et al.*,
220 2012]. The uncertainty range in Cloudsat IWP assigned by *Jiang et al.* [2012] is between
221 50% and a factor of two depending whether or not columns that the cloud radar has
222 identified as precipitating are excluded from the dataset. Ultimately, this wide variability
223 in the IWP that can be consistent with observations means that GCMs are left with
224 relatively little observational constraint in the creation of cloud parameterizations.
225 Evidently GCM mixed-phase parameterizations play an important role in determining the
226 column-integrated ice and liquid in mixed-phase regions. Does this matter to the SW
227 cloud feedback? In general, it appears that models whose mixed-phase clouds contain a
228 greater amount of ice that is susceptible to transitioning to water will have a larger
229 increase in liquid water with warming. This is shown in Figure 4 by examining the
230 change in LWP for a CO₂-induced warming, where the change in LWP has been
231 normalized by surface temperature change.

232 Figure 4 shows that the intermodel spread in T5050 is strongly correlated with
233 warming-induced increases in LWP. That is to say, models that glaciate their cloud cover

234 more at warmer temperatures also increase their LWP more strongly in a warming
235 climate and have a more pronounced negative optical depth feedback.

236 <<Insert Figure 4 here>>

237 The first intercomparison of GCM mixed-phase cloud feedbacks was performed
238 by *Tsushima et al.* [2006], who analyzed five of the GCMs participating in the third
239 climate model intercomparison project (CMIP3) and showed that there was a strong
240 relationship between the phase partitioning in mixed-phase clouds and warming-induced
241 increases in LWP. This dependence of the optical depth feedback on ice and liquid
242 partitioning was also demonstrated by *Choi et al.* [2014], who created several versions of
243 the CAM3 GCM with different ice and liquid partitioning functions. This behavior still
244 appears to be a robust feature of CMIP5 models [*McCoy et al.*, 2015a]. *Ceppi et al.*
245 [2016a] further demonstrated that this linkage is causal and not coincidental by
246 perturbing the mixed-phase microphysical parameterizations in GFDL-AM2.1 and
247 CESM-CAM5 showing that decreased efficiency of liquid water sinks through mixed-
248 phase processes played a critical role in the increase in mid-latitude LWP with warming.
249 It is interesting to note that there is not a consensus between GCMs participating in
250 CMIP5 regarding whether the increase in LWP with warming is dominated by a simple
251 repartitioning of condensate with warming, or if it is due to an increase in overall
252 condensate mass in line with decreases in precipitation efficiency [*Ceppi et al.*, 2016a;
253 *McCoy et al.*, 2015a]. In some GCMs the increase in LWP with warming may be
254 explained entirely by replacing ice with liquid in line with increasing atmospheric
255 temperature and the curves shown in Figure 2, while the increase in LWP in other GCMs
256 is almost entirely due to increases in overall cloud condensate in line with suppression of
257 frozen precipitation sinks as clouds move to a less glaciated state [*McCoy et al.*, 2015a].
258 Because of this model diversity, observations of changes in precipitation efficiency due
259 to changes in prevalence of glaciated hydrometeors may be a useful constraint on the
260 mixed-phase cloud feedback.

261 Viewing mixed-phase cloud properties in a zonal-mean sense is useful for
262 discussing the large spread in cloud feedbacks in the Southern Ocean among GCMs.
263 However, in order to provide more realistic model parameterization of mixed-phase cloud
264 processes it is important to investigate how different cloud regimes contribute to the

265 mixed-phase cloud feedback. Studies based on cyclone compositing in mid-latitude
266 regions reveal that the change in LWP with warming and changes in reflected SW are not
267 tightly coupled [*Bodas-Salcedo et al.*, 2016]. The clouds in cyclone composites that are
268 responsible for the bulk of the radiative response to warming are non-frontal clouds,
269 which are relatively thin and tend to be supercooled liquid, as opposed to the frontal
270 clouds, which have significant amount of ice and liquid. Because the frontal clouds are
271 already relatively opaque, increases in their optical depth are less important than
272 increases in the optical depth of thin, non-frontal clouds [*Bodas-Salcedo et al.*, 2016].

273 Discussion of the mixed-phase cloud feedback tends to focus on mixed-, and ice-
274 phase microphysics, but warm, liquid microphysics also have the potential to affect the
275 mixed-phase cloud feedback. We have discussed the mixed-phase cloud feedback in the
276 context of changes in LWP. However, cloud optical depth is controlled by both LWP and
277 cloud droplet number concentration, which is in turn controlled by the availability of
278 cloud condensation nuclei (CCN) [*Bréon et al.*, 2002; *Nakajima et al.*, 2001; *Sekiguchi et*
279 *al.*, 2003; *Storelvmo et al.*, 2006; *Twomey*, 1977]. It is interesting to speculate on how
280 changes in the availability of cloud condensation nuclei (CCN) with warming will affect
281 the mixed-phase cloud feedback. As noted before, liquid droplets are much smaller than
282 ice-crystals, and thus a given mass of cloud liquid is brighter than the same mass of ice.
283 However, the availability of CCN, and thus the number concentration in the deglaciated
284 cloud, also significantly affects the strength of the mixed-phase cloud feedback by
285 affecting how relatively bright the newly minted liquid is [*McCoy et al.*, 2014]. The
286 mixed-phase cloud feedback occurs in both the Northern and Southern midlatitudes.
287 These are extremely different aerosol regimes. In the Northern Hemisphere
288 anthropogenic CCN controls cloud microphysical properties [*Carslaw et al.*, 2013]. The
289 Southern Ocean is highly pristine and accurate representation of its aerosol sources is
290 difficult [*Hamilton et al.*, 2014]. Sources of CCN in the Southern Ocean are primarily
291 natural and composed of sea spray and the sulfate from biogenic dimethyl sulfide (DMS)
292 [*G. P. Ayers and Gras*, 1991; *Greg P. Ayers and Cainey*, 2007; *Charlson et al.*, 1987;
293 *Kruger and Grassl*, 2011; *Lana et al.*, 2012; *McCoy et al.*, 2015b; *Meskhidze and Nenes*,
294 2006; 2010; *Vallina and Simó*, 2007; *Vallina et al.*, 2006]. Because a complex web of
295 organisms produces DMS it is difficult to precisely diagnose how changes in the ocean

296 biome will affect its production. It seems likely that biogenic emissions of DMS will
297 decrease with increasing ocean acidification in a warming world [*Six et al.*, 2013],
298 potentially blunting the negative mid-latitude mixed-phase cloud feedback. The control
299 of Southern Ocean CCN by sea-spray aerosol is particularly interesting because sea spray
300 emissions are closely tied to wind speed [*Grythe et al.*, 2014], and mixed-phase cloud
301 parameterizations will affect wind speed through their control of the latitudinal gradient
302 of absorbed SW radiation [*Ceppi et al.*, 2014; *McCoy et al.*, 2016], potentially yielding an
303 interplay of these mechanisms.

304 Ultimately, the amount of liquid in a cloud plays a central role in determining its
305 albedo. If the LWP in mixed-phase regions is so strongly controlled by the mixed-phase
306 parameterization in a given GCM there must be another factor to counter-balance it and
307 bring the planetary albedo into a reasonable agreement with observations. That is to say,
308 the planetary albedo in a given GCM should be approximately consistent with
309 observational estimates in the climate mean-state. If too little supercooled liquid is
310 maintained in the clouds then this will lead to too low an albedo. Some other factor must
311 increase the planetary albedo so that it is generally consistent with observations. It
312 appears that, at least in the most recent generation of GCMs, this factor is the cloud
313 fraction. It can be seen by regressing inter-model spread in cloud fraction on the mixed-
314 phase characterization parameter, T5050, that models that glaciate clouds at warmer
315 temperatures (higher T5050) both have lower LWP and a higher CF [*McCoy et al.*, 2016].
316 The correlation between T5050 and LWP is restricted to regions where a substantial
317 amount of cloud exists above the melting level, but the inter-model correlation between
318 T5050 and cloud area coverage appears to be a global phenomenon, which is clearly
319 unphysical, especially since one would expect increased glaciation to decrease cloud
320 cover [*Heymsfield et al.*, 2009; *McCoy et al.*, 2016]. One possible explanation of this
321 behavior is that the critical relative humidity (RH) that GCMs use to parameterize cloud
322 cover [*Bender*, 2008; *Mauritsen et al.*, 2012; *Quaas*, 2012] is adjusted to increase cloud
323 cover and thus bring planetary albedo into a reasonable range. This is not an entirely
324 unreasonable supposition and has been singled out as a common ‘tuning parameter’
325 [*Bender*, 2008; *Mauritsen et al.*, 2012]. Anecdotally, it may be seen that in studies which
326 have directly addressed the sensitivity of Southern Ocean cloud properties to mixed-

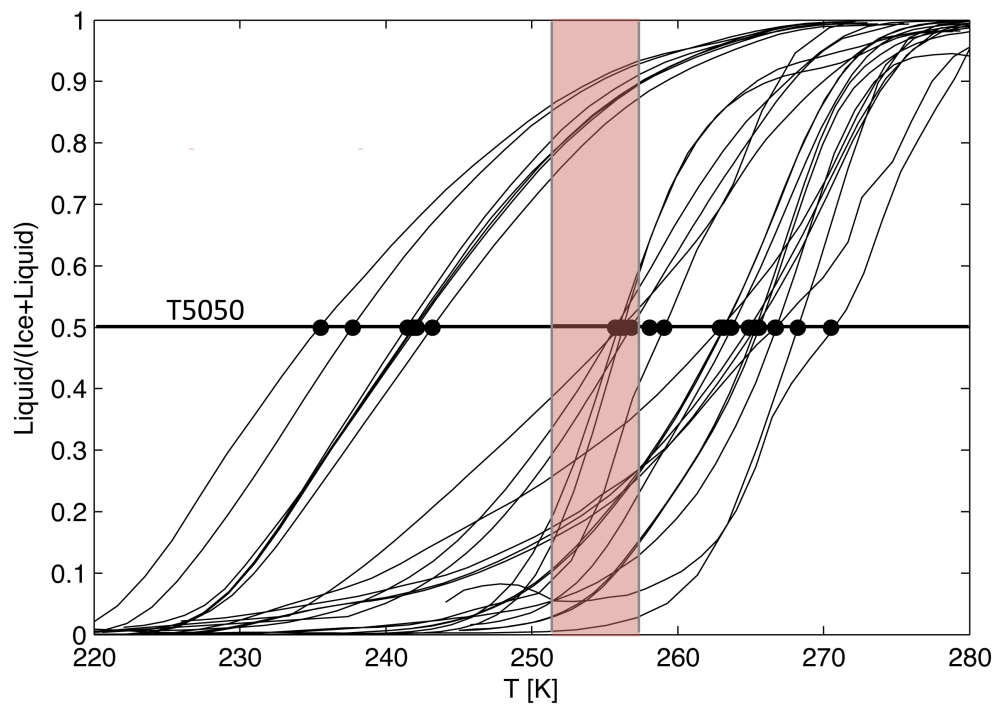
327 phase parameterizations that the critical RH has been adjusted to yield a control climate
328 that is in energy balance [*Kay et al.*, 2016; *Tan et al.*, 2016]. Ultimately, this tuning
329 between mixed-phase clouds and cloud fraction yields brighter subtropics and darker
330 extratropics when model clouds glaciate at warmer temperatures [*McCoy et al.*, 2016]. It
331 is interesting to note that this behavior is consistent with the emergent constraint on ECS
332 offered by *Volodin* [2008] (see *Klein and Hall* [2015] for a discussion of emergent
333 constraints).

334 In mixed-phase regions this tuning between cloud cover and liquid content in
335 MPCs also results in clouds that are both too few, or cover too little area, and clouds that
336 contain too much liquid and are too bright. In many GCMs this seesaw between cloud
337 liquid and cloud area yields model cloud properties that agree poorly with observed cloud
338 properties [*McCoy et al.*, 2016].

339 The choices made regarding mixed-phase cloud parameterizations in GCMs have
340 far ranging impacts on model behavior. Can we use observations of mixed-phase cloud
341 temperature range to provide a so-called emergent constraint [*Klein and Hall*, 2015] on
342 climate sensitivity in the current generation of GCMs? The T5050 that characterizes
343 mixed-phase cloud parameterization does not correlate strongly across models with
344 equilibrium climate sensitivity [*McCoy et al.*, 2016]. This is because the subtropical
345 cloud area feedback is more positive in models with a higher T5050, effectively
346 counterbalancing the more negative cloud optical depth feedback in the midlatitudes
347 (higher T5050 implies stronger increase in LWP with warming, see Figure 4). It is not
348 clear why models with a higher T5050 have a more positive subtropical cloud amount
349 feedback. One potential mechanism may be the positive feedbacks between boundary-
350 layer radiative cooling, relative humidity, and cloud cover, as described by *Brient and*
351 *Bony* [2013], thus linking climate mean-state cloud fraction to the response of cloud
352 fraction to warming.

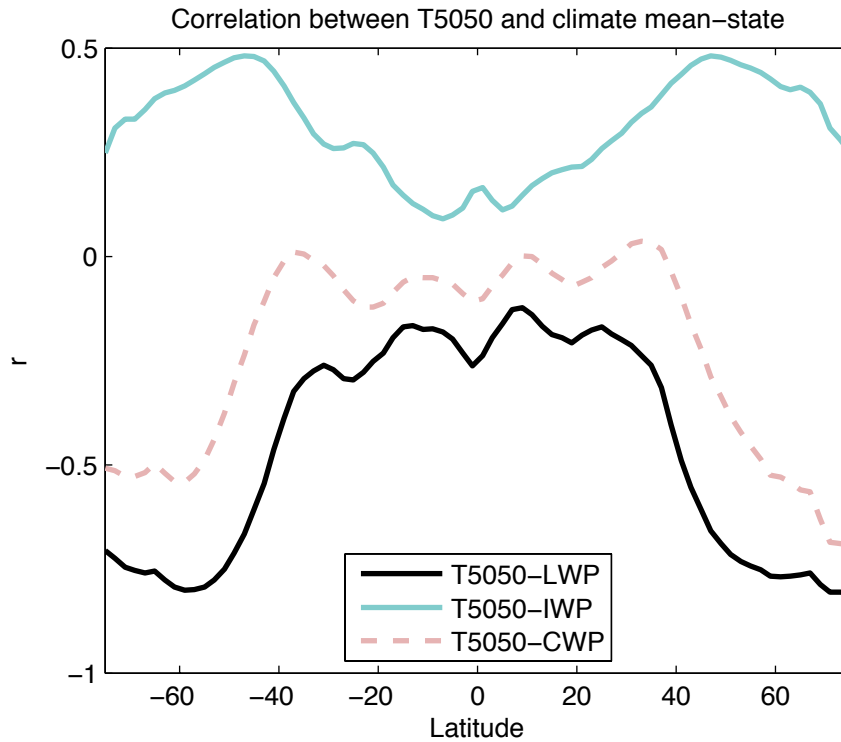
353 In summary, because of the wide variety of mixed-phase cloud behavior in the
354 current GCMs cloud optical depth feedbacks are highly uncertain. However, GCMs must
355 have a reasonable planetary albedo. Because of this necessity, uncertainty as to the
356 amount of liquid in mixed-phase cloud cover results in a counterbalancing variability in
357 cloud area. This seesaw between cloud area and mixed-phase cloud liquid results in

358 cancellation between the negative optical depth feedback in the mid-latitudes and the
 359 positive cloud area feedback in the subtropics. Investigation by *Zelinka et al.* [2016] in
 360 CMIP3 and CMIP5 GCMs that provided ISCCP simulator output showed a 17% decrease
 361 in intermodel variance in net cloud feedback due to this anti-correlation between cloud
 362 amount and optical depth feedback. Given the robustness of the positive subtropical
 363 cloud area feedback (see introduction) it is probable that this compensation between
 364 cloud amount and optical depth feedbacks leads to an underestimation of climate
 365 sensitivity in the current generation of GCMs. In the next section we will discuss
 366 observational constraints on the mixed-phase cloud feedback.



367
 368 **Figure 2** The fraction of cloud water that is liquid as a function of atmospheric temperature from a
 369 selection of GCMs participating in CMIP5 (for a full list of GCMs and details of the calculation see *McCoy et*
 370 *al.* [2015a]). The midpoint of the curves, where ice and liquid are equally mixed (T5050), is shown
 371 highlighted by dots. The range in of T5050 that would be inferred based on the CALIPSO cloud top phase
 372 [*Hu et al., 2010*] combined with comparison between partitioning and simulated lidar data from *Cesana*
 373 *et al.* [2015]; [*Hu et al., 2010*] is shown in red.

374



375

376

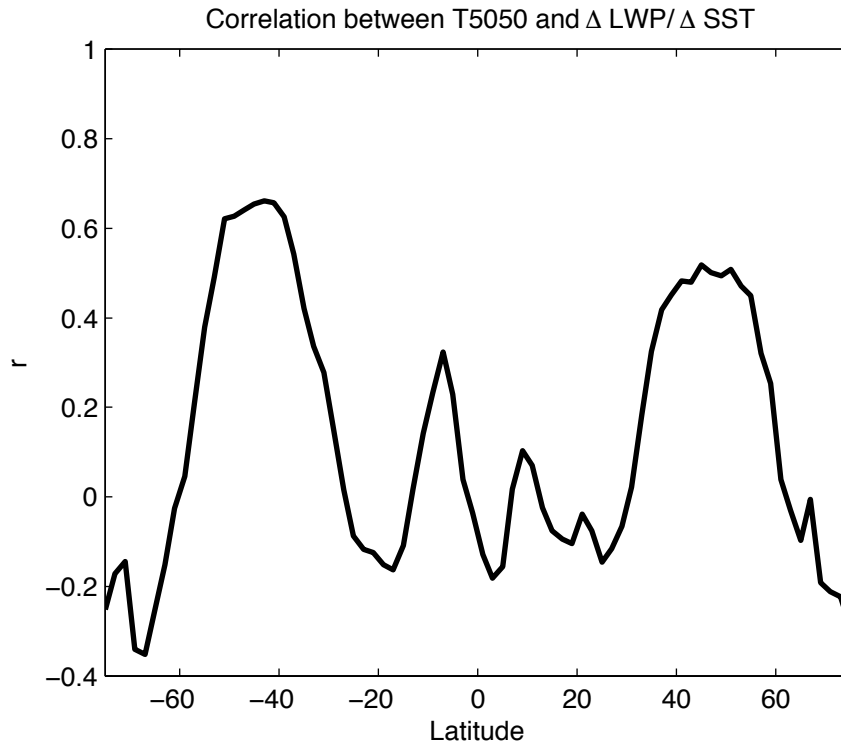
377

378

379

380

Figure 3 The across model correlation between T5050 (see Figure 2) and zonal-mean climate mean-state cloud properties over oceans: liquid water path (LWP), ice water path (IWP), and ice and liquid, or condensed water path (CWP). In the mid-latitudes, GCMs that freeze liquid at warmer temperatures (high T5050) have less liquid and more ice. They also have less overall ice and liquid water path. (Figure adapted from McCoy *et al.* [2016]).



381

382 **Figure 4 as in Figure 3, but showing the correlation between T5050 and change in zonal-mean LWP over**
 383 **oceans normalized by change in SST between historical and RCP8.5 scenarios in CMIP5. GCMs that have a**
 384 **mixed-phase scheme that has generated a large amount of susceptible ice in the climate mean state**
 385 **increase their liquid water path more with warming.**

386

387

388 **Observations of the mixed-phase cloud feedback**

389 In the previous sections we have discussed the mixed-phase cloud feedback in the
 390 context of climate models. Can we observe the fingerprint of the mixed-phase cloud
 391 feedback in the observational record?

392 This task is somewhat hampered by the fact that the negative optical depth
 393 feedback should occur in the high- and mid-latitudes. Passive remote sensing is subject
 394 to substantial errors at low sun angles in the high-latitude wintertime [*Grosvenor and*
 395 *Wood, 2014*]. Further, the longer data records offered by ISCCP [*Rossow and Schiffer,*

396 1999] and PATMOS-x [Heidinger et al., 2014] are not stable in a climate sense and must
397 be corrected for artifacts [Norris and Evan, 2015].

398 Even with these observational uncertainties, can we see optical depth increasing
399 with increasing surface temperature in the satellite record? Several studies have shown a
400 pronounced increase in optical depth with warming over land at low temperatures
401 [Feigelson, 1978; Genio and Wolf, 2000; Tselioudis et al., 1992] while studies over ocean
402 regions generally indicate no covariance between warming and optical depth, or a slight
403 decrease [Norris and Iacobellis, 2005; Tselioudis et al., 1992]. Gordon and Klein [2014]
404 demonstrated that by comparing the optical depth feedback in GCMs with the optical
405 depth-temperature relation detected by Tselioudis et al. [1992] that the strong negative
406 cloud feedback diagnosed by GCMs was too negative.

407 Is there no evidence of a substantial increase in cloud optical depth with warming
408 over oceans? The difficulty in robustly detecting an increase optical depth with increasing
409 surface temperature in the observational record may reflect observational limitations, but
410 it may also be partially due to the fact that many different mechanisms affect boundary-
411 layer maritime cloud cover in a warming world. As noted earlier, cloud amount, and to
412 some extent LWP, should generally decrease with enhanced surface temperature in the
413 absence of mixed-phase transitions [Bretherton and Blossey, 2014], and it should
414 increase due to increased boundary layer stability, which increases with surface
415 temperature [Klein and Hartmann, 1993; Myers and Norris, 2015; Qu et al., 2014a; b; Qu
416 et al., 2015; Wood and Bretherton, 2006]. Given the limited resolution of remote-sensing
417 instruments, observational artifacts engendered by attempting to disentangle changes in
418 cloud area from cloud optical depth may potentially make detecting the sensitivity of
419 cloud albedo to temperature difficult.

420 Despite these issues, recent investigation directed at exploring the possibility of a
421 negative cloud feedback due to mixed phase transitions have diagnosed a near-zero to
422 weak increase in cloud optical depth with temperature. While these studies disagree
423 somewhat as to the strength of the midlatitude SW cloud feedback, they agree that the
424 most negative SW cloud feedbacks in GCMs are not consistent with the current
425 observational record [Ceppi et al., 2016b; Terai et al., 2016].

426 The observationally constrained range of the Southern Ocean SW cloud feedback
427 (including both amount and optical depth components) inferred by *Ceppi et al.* [2016b] is
428 more negative than the range inferred by *Terai et al.* [2016], even though these studies
429 share observational data sets. It is probable that this difference is due to systematic
430 differences in the approaches taken by these studies to diagnosing the sensitivity of cloud
431 optical depth to temperature. Different predictor variables may partially explain the
432 different results arrived at by these studies. *Ceppi et al.* [2016b] regressed upon low- to
433 mid-tropospheric temperature alone, while *Terai et al.* [2016] regressed upon both
434 estimated inversion strength (EIS, [*Wood and Bretherton*, 2006]) and temperature.
435 Strong and nonlinear covariation between EIS and tropospheric temperature [*Myers and*
436 *Norris*, 2015] may lead to attributing variation in optical depth and cloud cover to
437 tropospheric temperature that are due to variation in EIS if only temperature is used as a
438 predictor. Another possible source of disagreement between these studies is that *Terai et*
439 *al.* [2016] focused on the optical depth of low clouds, while *Ceppi et al.* [2016b]
440 investigated changes in both cloud fraction and optical depth without restricting to low
441 clouds. [*Ceppi et al.*, 2016b] diagnosed increases in both cloud cover and optical depth
442 with warming leading to a negative overall SW cloud feedback. For these studies to be
443 compared they must both be cast in terms of the SW cloud feedback as a whole. When
444 *Terai et al.* [2016] replaced the optical depth portion of the SW cloud feedback in GCMs
445 with the optical depth sensitivities that they diagnosed from observations their results
446 were in agreement with the overall SW cloud feedback range inferred by *Ceppi et al.*
447 [2016b]. This is summarized in Figure 5 for the Southern Ocean in the latitude band
448 45°S-60°S.

449 << Insert Figure 5 here >>

450 Ultimately, it appears that the observational record is in qualitative agreement that
451 the most negative SW cloud feedbacks predicted by GCMs are too negative (Figure 5).
452 This result is consistent with the results presented in the previous section: compared to
453 observations, GCMs generally represent mixed-phase clouds as too glaciated at warm
454 temperatures and increase LWP with warming too strongly. This too-strong dependence
455 of LWP on temperature is corroborated by investigation of the long data record of
456 microwave-observed LWP [*O'Dell et al.*, 2008] shown in *Ceppi et al.* [2016b]. The

457 dependence of LWP on temperature derived in this study is shown in Figure 6. This
458 provides a complimentary analysis to studies investigating the dependence of optical
459 depth on temperature because optical depth is a function of both droplet number
460 concentration and liquid water path. Showing that LWP is dependent on surface
461 temperature disentangles possible trends in cloud microphysical properties.

462 <<Insert Figure 6 here>>

463

464 **Constraint of Mixed-Phase properties in GCMs**

465 Evidently the mixed-phase optical depth feedback is consistent with the
466 observational record. As discussed above, the decisions that GCMs make concerning the
467 handling of mixed-phase cloud cover strongly affects the negative optical depth feedback.
468 Because of the pronounced hemispheric contrast in IN and, subsequently cloud
469 glaciation [Hu et al., 2010; Kanitz et al., 2011; Tan et al., 2014], GCMs should have a
470 parameterization that responds to aerosol concentrations to properly represent mixed-
471 phase cloud cover. One way to pursue this is to attempt to simply create the most
472 advanced parameterization possible, but due to the complexity of mixed-phase cloud
473 microphysics this has been exceedingly difficult to accomplish. Some processes that
474 govern the mixed-phase system simply lack any strong observational constraint and they
475 may be thought of as a so-called ‘tunable-parameter’ [Tan and Storelmo, 2016].

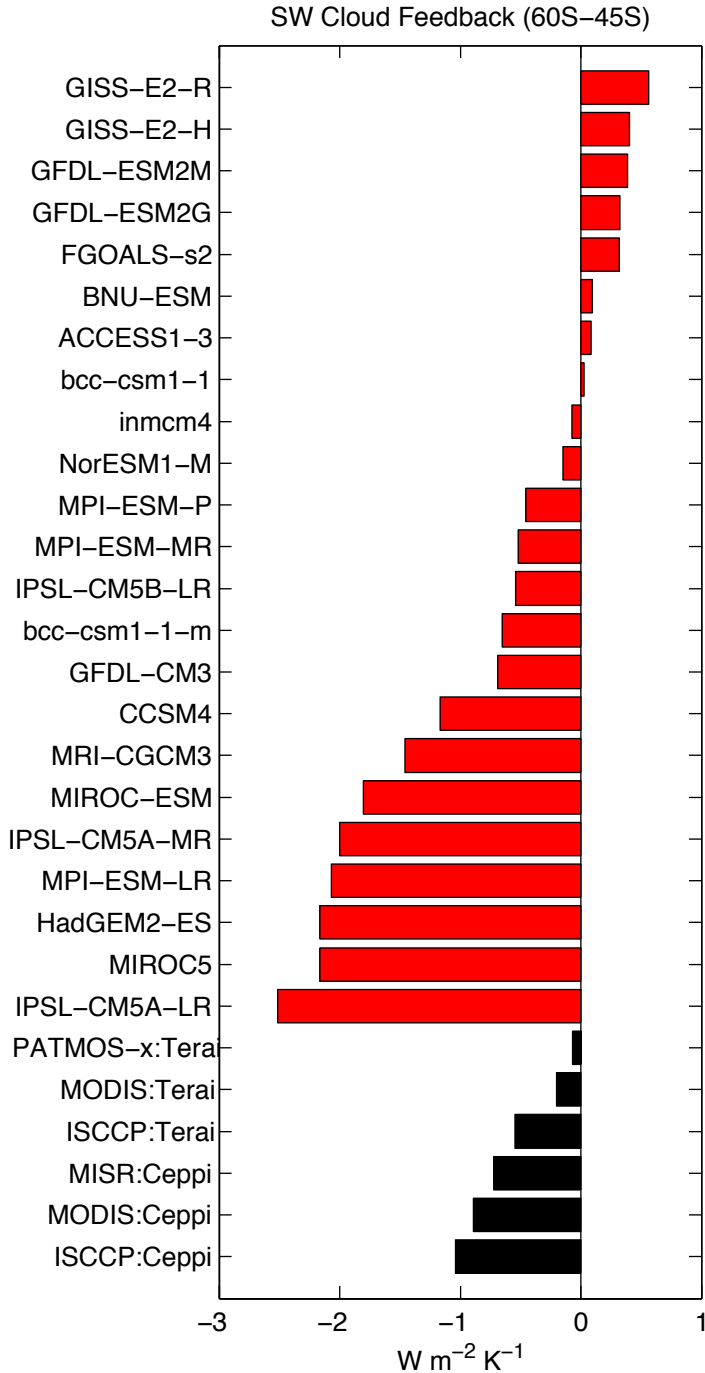
476 Ultimately, the goal of adjusting the mixed-phase parameterization is to improve
477 model biases in regional radiation budgets, and the global circulation [Grise et al., 2015;
478 Kay et al., 2016; Trenberth and Fasullo, 2010]. One approach that has been used to
479 address uncertainty in how to adjust the mixed-phase parameterization is to choose the
480 parameters that govern mixed-phase clouds in GCMs in such a way that the simulated
481 CALIPSO supercooled liquid occurrence in the GCM matches observations [Tan and
482 Storelmo, 2016]. In prognostic mixed-phase parameterizations there are many different
483 factors that control the occurrence of supercooled liquid and there are many different
484 combinations that may generate similar looking mixed-phase clouds. To explore this Tan
485 and Storelmo [2016] utilized a quasi-Monte Carlo sampling approach to investigate how
486 different combinations of mixed-phase parameters satisfied observational constraints on

487 supercooled liquid occurrence. In the sensitivity analysis conducted by *Tan and*
488 *Storelvmo* [2016] it was found that the vast majority of supercooled liquid occurrence in
489 the CAM5.1 GCM was governed by the Wegener-Bergeron-Findeisen (WBF) process
490 [*Storelvmo and Tan*, 2015]. The importance of the WBF process inferred by *Tan and*
491 *Storelvmo* [2016] is in agreement with the investigations of existing GCM
492 parameterizations conducted by *Cesana et al.* [2015] and *Komurcu et al.* [2014], which
493 also found that the WBF process exerted a significant control on the mixed-phase cloud
494 behavior in an array of different GCMs. The version of CAM5.1 created by *Tan and*
495 *Storelvmo* [2016] to agree best with CALIPSO was run with the fully-coupled version of
496 the model in *Tan et al.* [2016] to investigate the response of the model to warming. It was
497 found that this adjustment to bring the mixed-phase cloud parameterization into
498 agreement with observed supercooled liquid occurrence raised the equilibrium climate
499 sensitivity (ECS) substantially as it reduced the occurrence of glaciated cloud cover in the
500 climate mean-state and reduced the negative mid-latitude optical depth cloud feedback.

501 The creation of a mixed-phase cloud scheme that is tuned to agree with our best
502 space-borne measures of mixed-phase behavior in a state-of-the-art GCM substantially
503 increases the ECS within that model. What does this mean for the range on ECS offered
504 by model intercomparison? It should be noted that many other factors determine the ECS
505 of a given GCM. However, the increase in CESM's ECS in *Tan et al.* [2016]'s analysis
506 indicates that misrepresentation of mixed-phase clouds had led to an under-representation
507 of ECS within that model. As noted earlier, in general, GCMs tend to glaciate mixed-
508 phase clouds at temperatures that are too warm in the global-mean relative to space-borne
509 estimates [*Cesana et al.*, 2015; *McCoy et al.*, 2016]. Tighter constraints on the mixed-
510 phase parameterizations in these GCMs should lead to an increase in ECS in models with
511 too little supercooled liquid as the magnitude of the mixed-phase cloud feedback is
512 reduced.

513

514



515

516

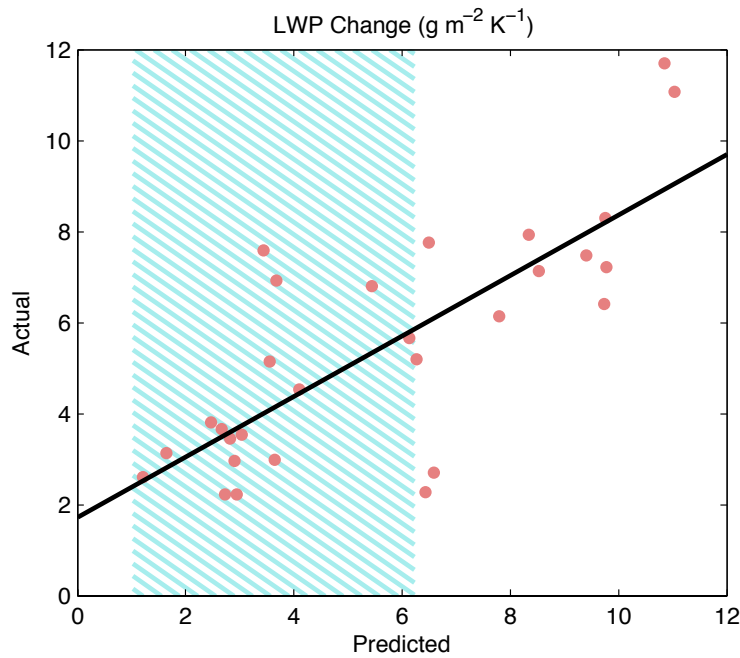
517

518

519

Figure 5 SW cloud feedback from GCMs participating in CMIP5 (see *Zelinka et al. [2013]*) (red) compared to observationally constrained estimates of the SW cloud feedback from *Ceppi et al. [2016b]* and *Terai et al. [2016]* (black). Averages are taken over the latitude band between 45°S and 60°S.

520



521

522 **Figure 6 LWP change in GCMs predicted by their temperature sensitivity versus their response to**
523 **warming. The observational range inferred from long-term microwave measurements of LWP is**
524 **indicated using cross-hatching. (Adapted from Ceppi et al. [2016b]).**

525

526 **Summary**

527 In this chapter we have discussed the negative cloud optical depth feedback that
528 appears across GCMs in middle to high latitudes. This feedback is due to mixed-phase
529 clouds transitioning to a less glaciated state as the planet warms. The uncertainty in the
530 mixed-phase cloud feedback results from the wide variety of mixed-phase
531 parameterizations that exist in the current generation of GCMs. Models that glaciate at
532 warmer temperatures have a larger reservoir of ice in their mixed phase cloud cover that
533 is susceptible to warming, which transitions to liquid as the climate warms and produce a
534 stronger negative optical depth feedback. Cloud fraction is higher in models that glaciate
535 clouds at warmer temperatures. This appears to be a result of the fact that a good fit to the
536 observed cloud reflectivity is a product of cloud fraction and cloud optical depth. If
537 models have more ice and thus a lower cloud optical depth, then they must have a higher
538 cloud fraction to produce a realistic planetary albedo. This indirect control of cloud cover

539 by the mixed-phase parameterizations in GCMs also produce an artifact of cancellation
540 between subtropical positive cloud feedback and midlatitude negative cloud feedback.
541 (Figure 1).

542 We discuss several recent papers that use the satellite observational record to
543 evaluate the strength of the mixed-phase cloud feedback. These studies agree in
544 diagnosing a cloud feedback in the mid-latitudes due to cloud optical depth changes that
545 is either weakly negative or near zero. Overall, they agree in showing that many GCMs
546 have SW cloud feedbacks that are too negative in the Southern Ocean (Figure 5)[*Ceppi et*
547 *al.*, 2016b; *Terai et al.*, 2016]. We have also discussed studies that evaluate the mixed-
548 phase temperature range in the current generation of GCMs. It was found that GCMs are
549 generally unable to maintain supercooled liquid to low enough temperatures. Because of
550 this GCMs generally over-represent the strength of the negative midlatitude cloud optical
551 depth feedback [*McCoy et al.*, 2016]. This is also in agreement with evaluations made
552 using a state of the art GCM that has had its mixed-phase parameterization constrained to
553 better agree with space-borne observations of super-cooled liquid cloud occurrence [*Tan*
554 *et al.*, 2016].

555 The representation of mixed-phase clouds in GCMs is important to the accurate
556 prediction of 21st century climate change and to accurately represent the current climate.
557 Overall, it is likely that this too-strong negative cloud optical depth feedback leads to an
558 underestimation of climate sensitivity. Based on these different lines of investigation it
559 seems clear that GCMs must carefully vet their mixed-phase parameterizations so that
560 they agree, at least roughly, with observations of mixed-phase clouds.

561

562 **Acknowledgements**

563 The authors wish to thank Ivy Tan for useful discussion and advice during the preparation
564 of this chapter. The authors acknowledge funding under DOE grant DE-SC0012580 and
565 DTM and DLH acknowledge funding under NASA grant NNX14AJ26G. The effort of
566 MDZ was performed under the auspices of the U.S. Department of Energy by Lawrence
567 Livermore National Laboratory under contract DE-AC52-07NA27344.

568

569

570

571

572 **References**

- 573 Atkinson, J. D., B. J. Murray, M. T. Woodhouse, T. F. Whale, K. J. Baustian, K. S.
574 Carslaw, S. Dobbie, D. O'Sullivan, and T. L. Malkin (2013), The importance of feldspar
575 for ice nucleation by mineral dust in mixed-phase clouds, *Nature*, 498(7454), 355-358.
576 Ayers, G. P., and J. L. Gras (1991), Seasonal relationship between cloud condensation
577 nuclei and aerosol methanesulphonate in marine air, *Nature*, 353(6347), 834-835.
578 Ayers, G. P., and J. M. Cainey (2007), The CLAW hypothesis: a review of the major
579 developments, *Environmental Chemistry*, 4(6), 366-374.
580 Bender, F. A. M. (2008), A note on the effect of GCM tuning on climate sensitivity,
581 *Environ. Res. Lett.*, 3(1), 014001.
582 Bender, F. A. M., V. Ramanathan, and G. Tselioudis (2011), Changes in extratropical
583 storm track cloudiness 1983-2008: observational support for a poleward shift, *Climate*
584 *Dynamics*, 38(9-10), 2037-2053.
585 Blossey, P. N., C. S. Bretherton, M. H. Zhang, A. N. Cheng, S. Endo, T. Heus, Y. G. Liu,
586 A. P. Lock, S. R. de Roode, and K. M. Xu (2013), Marine low cloud sensitivity to an
587 idealized climate change: The CGILS LES intercomparison, *J. Adv. Model. Earth Syst.*,
588 5(2), 234-258.
589 Bodas-Salcedo, A., T. Andrews, A. V. Karmalkar, and M. A. Ringer (2016), Cloud liquid
590 water path and radiative feedbacks over the Southern Ocean, *Geophys. Res. Lett.*, n/a-n/a.
591 Bony, S., et al. (2006), How well do we understand and evaluate climate change feedback
592 processes?, *Journal of Climate*, 19(15), 3445-3482.
593 Bower, K. N., S. J. Moss, D. W. Johnson, T. W. Choulaton, J. Latham, P. R. A. Brown,
594 A. M. Blyth, and J. Cardwell (1996), A parametrization of the ice water content observed
595 in frontal and convective clouds, *Quarterly Journal of the Royal Meteorological Society*,
596 122(536), 1815-1844.
597 Bréon, F.-M., D. Tanré, and S. Generoso (2002), Aerosol Effect on Cloud Droplet Size
598 Monitored from Satellite, *Science*, 295(5556), 834-838.
599 Bretherton, C. S. (2015), Insights into low-latitude cloud feedbacks from high-resolution
600 models, *Philosophical Transactions of the Royal Society of London A: Mathematical,*
601 *Physical and Engineering Sciences*, 373(2054).
602 Bretherton, C. S., and P. N. Blossey (2014), Low cloud reduction in a greenhouse-
603 warmed climate: Results from Lagrangian LES of a subtropical marine cloudiness
604 transition, *J. Adv. Model. Earth Syst.*, 6(1), 91-114.
605 Bretherton, C. S., P. N. Blossey, and C. R. Jones (2013), Mechanisms of marine low
606 cloud sensitivity to idealized climate perturbations: A single-LES exploration extending
607 the CGILS cases, *J. Adv. Model. Earth Syst.*, 5(2), 316-337.
608 Brient, F., and S. Bony (2013), Interpretation of the positive low-cloud feedback
609 predicted by a climate model under global warming, *Climate Dynamics*, 40(9-10), 2415-
610 2431.
611 Caldwell, P. M., Y. Y. Zhang, and S. A. Klein (2013), CMIP3 Subtropical Stratocumulus
612 Cloud Feedback Interpreted through a Mixed-Layer Model, *Journal of Climate*, 26(5),
613 1607-1625.
614 Carro-Calvo, L., C. Hoose, M. Stengel, and S. Salcedo-Sanz (2016), Cloud glaciation
615 temperature estimation from passive remote sensing data with evolutionary computing,
616 *Journal of Geophysical Research: Atmospheres*, n/a-n/a.

617 Carslaw, K. S., et al. (2013), Large contribution of natural aerosols to uncertainty in
618 indirect forcing, *Nature*, 503(7474), 67-71.

619 Ceppi, P., and D. Hartmann (2015), Connections Between Clouds, Radiation, and
620 Midlatitude Dynamics: a Review, *Curr Clim Change Rep*, 1(2), 94-102.

621 Ceppi, P., M. D. Zelinka, and D. L. Hartmann (2014), The response of the Southern
622 Hemispheric eddy-driven jet to future changes in shortwave radiation in CMIP5, *Geophys.*
623 *Res. Lett.*, 41(9), 3244-3250.

624 Ceppi, P., D. L. Hartmann, and M. J. Webb (2016a), Mechanisms of the Negative
625 Shortwave Cloud Feedback in Middle to High Latitudes, *Journal of Climate*, 29(1), 139-
626 157.

627 Ceppi, P., D. T. McCoy, and D. L. Hartmann (2016b), Observational evidence for a
628 negative shortwave cloud feedback in middle to high latitudes, *Geophys. Res. Lett.*, 43(3),
629 1331-1339.

630 Cesana, G., D. E. Waliser, X. Jiang, and J. L. F. Li (2015), Multi-model evaluation of
631 cloud phase transition using satellite and reanalysis data, *Journal of Geophysical*
632 *Research: Atmospheres*, n/a-n/a.

633 Charlson, R. J., J. E. Lovelock, M. O. Andreae, and S. G. Warren (1987), OCEANIC
634 PHYTOPLANKTON, ATMOSPHERIC SULFUR, CLOUD ALBEDO AND CLIMATE,
635 *Nature*, 326(6114), 655-661.

636 Choi, Y. S., C. H. Ho, C. E. Park, T. Storelvmo, and I. Tan (2014), Influence of cloud
637 phase composition on climate feedbacks, *Journal of Geophysical Research-Atmospheres*,
638 119(7), 3687-3700.

639 Clement, A. C., R. Burgman, and J. R. Norris (2009), Observational and Model Evidence
640 for Positive Low-Level Cloud Feedback, *Science*, 325(5939), 460-464.

641 Cober, S. G., G. A. Isaac, A. V. Korolev, and J. W. Strapp (2001), Assessing cloud-phase
642 conditions, *Journal of Applied Meteorology*, 40(11), 1967-1983.

643 Eliasson, S., S. A. Buehler, M. Milz, P. Eriksson, and V. O. John (2011), Assessing
644 observed and modelled spatial distributions of ice water path using satellite data, *Atmos.*
645 *Chem. Phys.*, 11(1), 375-391.

646 Feigelson, E. (1978), Preliminary radiation model of a cloudy atmosphere. I- Structure of
647 clouds and solar radiation, *Beitraege zur Physik der Atmosphaere*, 51(3), 203-229.

648 Field, P. R., and A. J. Heymsfield (2015), Importance of snow to global precipitation,
649 *Geophys. Res. Lett.*, 42(21), 9512-9520.

650 Genio, A. D. D., and A. B. Wolf (2000), The Temperature Dependence of the Liquid
651 Water Path of Low Clouds in the Southern Great Plains, *Journal of Climate*, 13(19),
652 3465-3486.

653 Gettelman, A., and S. C. Sherwood (2016), Processes Responsible for Cloud Feedback,
654 *Curr Clim Change Rep*, 1-11.

655 Gordon, N. D., and S. A. Klein (2014), Low-cloud optical depth feedback in climate
656 models, *Journal of Geophysical Research: Atmospheres*, 119(10), 6052-6065.

657 Grise, K. M., and B. Medeiros (2016), Understanding the Varied Influence of Midlatitude
658 Jet Position on Clouds and Cloud Radiative Effects in Observations and Global Climate
659 Models, *Journal of Climate*, 29(24), 9005-9025.

660 Grise, K. M., L. M. Polvani, and J. T. Fasullo (2015), Reexamining the Relationship
661 between Climate Sensitivity and the Southern Hemisphere Radiation Budget in CMIP
662 Models, *Journal of Climate*, 28(23), 9298-9312.

663 Grosvenor, D. P., and R. Wood (2014), The effect of solar zenith angle on MODIS cloud
664 optical and microphysical retrievals within marine liquid water clouds, *Atmos. Chem.*
665 *Phys.*, *14*(14), 7291-7321.

666 Grythe, H., J. Strom, R. Krejci, P. Quinn, and A. Stohl (2014), A review of sea-spray
667 aerosol source functions using a large global set of sea salt aerosol concentration
668 measurements, *Atmospheric Chemistry and Physics*, *14*(3), 1277-1297.

669 Hamilton, D. S., L. A. Lee, K. J. Pringle, C. L. Reddington, D. V. Spracklen, and K. S.
670 Carslaw (2014), Occurrence of pristine aerosol environments on a polluted planet,
671 *Proceedings of the National Academy of Sciences*, *111*(52), 18466-18471.

672 Hartmann, D. L., and D. A. Short (1980), On the Use of Earth Radiation Budget Statistics
673 for Studies of Clouds and Climate, *Journal of the Atmospheric Sciences*, *37*(6), 1233-
674 1250.

675 Heidinger, A. K., M. J. Foster, A. Walther, and X. Zhao (2014), The Pathfinder
676 Atmospheres–Extended AVHRR Climate Dataset, *Bulletin of the American*
677 *Meteorological Society*, *95*(6), 909-922.

678 Heymsfield, A. J., P. C. Kennedy, S. Massie, C. Schmitt, Z. Wang, S. Haimov, and A.
679 Rangno (2009), Aircraft-Induced Hole Punch and Canal Clouds: Inadvertent Cloud
680 Seeding, *Bulletin of the American Meteorological Society*, *91*(6), 753-766.

681 Hoose, C., and O. Möhler (2012), Heterogeneous ice nucleation on atmospheric aerosols:
682 a review of results from laboratory experiments, *Atmos. Chem. Phys.*, *12*(20), 9817-9854.

683 Hu, Y. X., S. Rodier, K. M. Xu, W. B. Sun, J. P. Huang, B. Lin, P. W. Zhai, and D. Josset
684 (2010), Occurrence, liquid water content, and fraction of supercooled water clouds from
685 combined CALIOP/IIR/MODIS measurements, *Journal of Geophysical Research-*
686 *Atmospheres*, *115*, 13.

687 Isaac, G. A., and R. S. Schemenauer (1979), Large Particles in Supercooled Regions of
688 Northern Canadian Cumulus Clouds, *Journal of Applied Meteorology*, *18*(8), 1056-1065.

689 Jiang, J. H., et al. (2012), Evaluation of cloud and water vapor simulations in CMIP5
690 climate models using NASA “A-Train” satellite observations, *Journal of Geophysical*
691 *Research: Atmospheres*, *117*(D14), D14105.

692 Kanitz, T., P. Seifert, A. Ansmann, R. Engelmann, D. Althausen, C. Casiccia, and E. G.
693 Rohwer (2011), Contrasting the impact of aerosols at northern and southern midlatitudes
694 on heterogeneous ice formation, *Geophys. Res. Lett.*, *38*, 5.

695 Kay, J. E., C. Wall, V. Yettella, B. Medeiros, C. Hannay, P. Caldwell, and C. Bitz (2016),
696 Global Climate Impacts of Fixing the Southern Ocean Shortwave Radiation Bias in the
697 Community Earth System Model (CESM), *Journal of Climate*, *29*(12), 4617-4636.

698 King, M. D., W. P. Menzel, Y. J. Kaufman, D. Tanre, G. Bo-Cai, S. Platnick, S. A.
699 Ackerman, L. A. Remer, R. Pincus, and P. A. Hubanks (2003), Cloud and aerosol
700 properties, precipitable water, and profiles of temperature and water vapor from MODIS,
701 *Geoscience and Remote Sensing, IEEE Transactions on*, *41*(2), 442-458.

702 Klein, S. A., and D. L. Hartmann (1993), The Seasonal Cycle of Low Stratiform Clouds,
703 *Journal of Climate*, *6*(8), 1587-1606.

704 Klein, S. A., and A. Hall (2015), Emergent Constraints for Cloud Feedbacks, *Curr Clim*
705 *Change Rep*, *1*(4), 276-287.

706 Klein, S. A., D. L. Hartmann, and J. R. Norris (1995), On the Relationships among Low-
707 Cloud Structure, Sea Surface Temperature, and Atmospheric Circulation in the
708 Summertime Northeast Pacific, *Journal of Climate*, *8*(5), 1140-1155.

709 Komurcu, M., T. Storelvmo, I. Tan, U. Lohmann, Y. X. Yun, J. E. Penner, Y. Wang, X.
710 H. Liu, and T. Takemura (2014), Intercomparison of the cloud water phase among global
711 climate models, *Journal of Geophysical Research-Atmospheres*, 119(6), 3372-3400.
712 Korolev, A., and G. Isaac (2003), Phase transformation of mixed-phase clouds, *Quarterly*
713 *Journal of the Royal Meteorological Society*, 129(587), 19-38.
714 Kruger, O., and H. Grassl (2011), Southern Ocean phytoplankton increases cloud albedo
715 and reduces precipitation, *Geophys. Res. Lett.*, 38.
716 Lana, A., R. Simo, S. M. Vallina, and J. Dachs (2012), Potential for a biogenic influence
717 on cloud microphysics over the ocean: a correlation study with satellite-derived data,
718 *Atmospheric Chemistry and Physics*, 12(17), 7977-7993.
719 Li, Z.-X., and H. Le Treut (1992), Cloud-radiation feedbacks in a general circulation
720 model and their dependence on cloud modelling assumptions, *Climate Dynamics*, 7(3),
721 133-139.
722 Mauritsen, T., et al. (2012), Tuning the climate of a global model, *J. Adv. Model. Earth*
723 *Syst.*, 4(3), n/a-n/a.
724 McCoy, D. T., D. L. Hartmann, and D. P. Grosvenor (2014), Observed Southern Ocean
725 Cloud Properties and Shortwave Reflection. Part II: Phase Changes and Low Cloud
726 Feedback, *Journal of Climate*, 27(23), 8858-8868.
727 McCoy, D. T., D. L. Hartmann, M. D. Zelinka, P. Ceppi, and D. P. Grosvenor (2015a),
728 Mixed-phase cloud physics and Southern Ocean cloud feedback in climate models,
729 *Journal of Geophysical Research: Atmospheres*, 120(18), 9539-9554.
730 McCoy, D. T., I. Tan, D. L. Hartmann, M. D. Zelinka, and T. Storelvmo (2016), On the
731 relationships among cloud cover, mixed-phase partitioning, and planetary albedo in
732 GCMs, *J. Adv. Model. Earth Syst.*, n/a-n/a.
733 McCoy, D. T., S. M. Burrows, R. Wood, D. P. Grosvenor, S. M. Elliott, P.-L. Ma, P. J.
734 Rasch, and D. L. Hartmann (2015b), Natural aerosols explain seasonal and spatial
735 patterns of Southern Ocean cloud albedo, *Science Advances*, 1(6).
736 Meskhidze, N., and A. Nenes (2006), Phytoplankton and Cloudiness in the Southern
737 Ocean, *Science*, 314(5804), 1419-1423.
738 Meskhidze, N., and A. Nenes (2010), Effects of Ocean Ecosystem on Marine Aerosol-
739 Cloud Interaction, *Advances in Meteorology*, 2010, 13.
740 Mitchell, J. F. B., C. A. Senior, and W. J. Ingram (1989), CO2 AND CLIMATE - A
741 MISSING FEEDBACK, *Nature*, 341(6238), 132-134.
742 Morrison, A. E., S. T. Siems, and M. J. Manton (2010), A Three-Year Climatology of
743 Cloud-Top Phase over the Southern Ocean and North Pacific, *Journal of Climate*, 24(9),
744 2405-2418.
745 Morrison, H., G. de Boer, G. Feingold, J. Harrington, M. D. Shupe, and K. Sulia (2011),
746 Resilience of persistent Arctic mixed-phase clouds, *Nature Geoscience*, 5(1), 11-17.
747 Moss, S. J., and D. W. Johnson (1994), Aircraft measurements to validate and improve
748 numerical model parametrisations of ice to water ratios in clouds, *Atmos. Res.*, 34(1-4), 1-
749 25.
750 Mossop, S. C., A. Ono, and E. R. Wishart (1970), Ice Particles In Maritime Clouds Near
751 Tasmania, *Quarterly Journal of the Royal Meteorological Society*, 96(409), 487-&.
752 Murray, B. J., D. O'Sullivan, J. D. Atkinson, and M. E. Webb (2012), Ice nucleation by
753 particles immersed in supercooled cloud droplets, *Chemical Society Reviews*, 41(19),
754 6519-6554.

755 Myers, T. A., and J. R. Norris (2013), Observational Evidence That Enhanced
756 Subsidence Reduces Subtropical Marine Boundary Layer Cloudiness, *Journal of Climate*,
757 26(19), 7507-7524.

758 Myers, T. A., and J. R. Norris (2015), On the Relationships between Subtropical Clouds
759 and Meteorology in Observations and CMIP3 and CMIP5 Models, *Journal of Climate*,
760 28(8), 2945-2967.

761 Myers, T. A., and J. R. Norris (2016), Reducing the uncertainty in subtropical cloud
762 feedback, *Geophys. Res. Lett.*, n/a-n/a.

763 Nakajima, T., A. Higurashi, K. Kawamoto, and J. E. Penner (2001), A possible
764 correlation between satellite-derived cloud and aerosol microphysical parameters,
765 *Geophys. Res. Lett.*, 28(7), 1171-1174.

766 Naud, C. M., A. D. Del Genio, and M. Bauer (2006), Observational constraints on the
767 cloud thermodynamic phase in midlatitude storms, *Journal of Climate*, 19(20), 5273-
768 5288.

769 Norris, J. R., and C. B. Leovy (1994), Interannual Variability in Stratiform Cloudiness
770 and Sea Surface Temperature, *Journal of Climate*, 7, 1915-1925.

771 Norris, J. R., and S. F. Iacobellis (2005), North Pacific Cloud Feedbacks Inferred from
772 Synoptic-Scale Dynamic and Thermodynamic Relationships, *Journal of Climate*, 18(22),
773 4862-4878.

774 Norris, J. R., and A. T. Evan (2015), Empirical Removal of Artifacts from the ISCCP and
775 PATMOS-x Satellite Cloud Records, *Journal of Atmospheric and Oceanic Technology*,
776 32(4), 691-702.

777 Norris, J. R., R. J. Allen, A. T. Evan, M. D. Zelinka, C. W. O'Dell, and S. A. Klein
778 (2016), Evidence for climate change in the satellite cloud record, *Nature, advance online
779 publication*.

780 O'Dell, C. W., F. J. Wentz, and R. Bennartz (2008), Cloud liquid water path from
781 satellite-based passive microwave observations: A new climatology over the global
782 oceans, *Journal of Climate*, 21(8), 1721-1739.

783 Qu, X., A. Hall, S. Klein, and P. Caldwell (2014a), On the spread of changes in marine
784 low cloud cover in climate model simulations of the 21st century, *Climate Dynamics*,
785 42(9-10), 2603-2626.

786 Qu, X., A. Hall, S. Klein, and P. Caldwell (2014b), The strength of the tropical inversion
787 and its response to climate change in 18 CMIP5 models, *Climate Dynamics*, 1-22.

788 Qu, X., A. Hall, S. A. Klein, DeAngelis, and M. Anthony (2015), Positive tropical marine
789 low-cloud cover feedback inferred from cloud-controlling factors, *Geophys. Res. Lett.*,
790 n/a-n/a.

791 Quaas, J. (2012), Evaluating the “critical relative humidity” as a measure of subgrid-scale
792 variability of humidity in general circulation model cloud cover parameterizations using
793 satellite data, *Journal of Geophysical Research: Atmospheres*, 117(D9), n/a-n/a.

794 Rieck, M., L. Nuijens, and B. Stevens (2012), Marine Boundary Layer Cloud Feedbacks
795 in a Constant Relative Humidity Atmosphere, *Journal of the Atmospheric Sciences*, 69(8),
796 2538-2550.

797 Rossow, W. B., and R. A. Schiffer (1999), Advances in understanding clouds from
798 ISCCP, *Bulletin of the American Meteorological Society*, 80(11), 2261-2287.

799 Seethala, C., J. R. Norris, and T. A. Myers (2015), How Has Subtropical Stratocumulus
800 and Associated Meteorology Changed since the 1980s?, *Journal of Climate*, 28(21),
801 8396-8410.

802 Sekiguchi, M., T. Nakajima, K. Suzuki, K. Kawamoto, A. Higurashi, D. Rosenfeld, I.
803 Sano, and S. Mukai (2003), A study of the direct and indirect effects of aerosols using
804 global satellite data sets of aerosol and cloud parameters, *Journal of Geophysical*
805 *Research: Atmospheres*, 108(D22), n/a-n/a.

806 Six, K. D., S. Kloster, T. Ilyina, S. D. Archer, K. Zhang, and E. Maier-Reimer (2013),
807 Global warming amplified by reduced sulphur fluxes as a result of ocean acidification,
808 *Nature Clim. Change*, 3(11), 975-978.

809 Storelmo, T., and I. Tan (2015), The Wegener-Bergeron-Findeisen process ? Its
810 discovery and vital importance for weather and climate, *Meteorologische Zeitschrift*,
811 24(4), 455-461.

812 Storelmo, T., I. Tan, and A. Korolev (2015), Cloud Phase Changes Induced by CO2
813 Warming—a Powerful yet Poorly Constrained Cloud-Climate Feedback, *Curr Clim*
814 *Change Rep*, 1(4), 1-9.

815 Storelmo, T., J. E. Kristjánsson, G. Myhre, M. Johnsrud, and F. Stordal (2006),
816 Combined observational and modeling based study of the aerosol indirect effect, *Atmos.*
817 *Chem. Phys.*, 6(11), 3583-3601.

818 Tan, I., and T. Storelmo (2016), Sensitivity Study on the Influence of Cloud
819 Microphysical Parameters on Mixed-Phase Cloud Thermodynamic Phase Partitioning in
820 CAM5, *Journal of the Atmospheric Sciences*, 73(2), 709-728.

821 Tan, I., T. Storelmo, and Y.-S. Choi (2014), Spaceborne lidar observations of the ice-
822 nucleating potential of dust, polluted dust, and smoke aerosols in mixed-phase clouds,
823 *Journal of Geophysical Research: Atmospheres*, n/a-n/a.

824 Tan, I., T. Storelmo, and M. D. Zelinka (2016), Observational constraints on mixed-
825 phase clouds imply higher climate sensitivity, *Science*, 352(6282), 224-227.

826 Terai, C. R., S. A. Klein, and M. D. Zelinka (2016), Constraining the low-cloud optical
827 depth feedback at middle and high latitudes using satellite observations, *Journal of*
828 *Geophysical Research: Atmospheres*, n/a-n/a.

829 Trenberth, K. E., and J. T. Fasullo (2010), Simulation of Present-Day and Twenty-First-
830 Century Energy Budgets of the Southern Oceans, *Journal of Climate*, 23(2), 440-454.

831 Tselioudis, G., W. B. Rossow, and D. Rind (1992), Global Patterns of Cloud Optical
832 Thickness Variation with Temperature, *Journal of Climate*, 5(12), 1484-1495.

833 Tsushima, Y., S. Emori, T. Ogura, M. Kimoto, M. J. Webb, K. D. Williams, M. A.
834 Ringer, B. J. Soden, B. Li, and N. Andronova (2006), Importance of the mixed-phase
835 cloud distribution in the control climate for assessing the response of clouds to carbon
836 dioxide increase: a multi-model study, *Climate Dynamics*, 27(2-3), 113-126.

837 Twomey, S. (1977), INFLUENCE OF POLLUTION ON SHORTWAVE ALBEDO OF
838 CLOUDS, *Journal of the Atmospheric Sciences*, 34(7), 1149-1152.

839 Vallina, S. M., and R. Simó (2007), Re-visiting the CLAW hypothesis, *Environmental*
840 *Chemistry*, 4(6), 384-387.

841 Vallina, S. M., R. Simo, and S. Gasso (2006), What controls CCN seasonality in the
842 Southern Ocean? A statistical analysis based on satellite-derived chlorophyll and CCN
843 and model-estimated OH radical and rainfall, *Global Biogeochemical Cycles*, 20(1).

844 Vial, J., J. L. Dufresne, and S. Bony (2013), On the interpretation of inter-model spread
845 in CMIP5 climate sensitivity estimates, *Climate Dynamics*, 41(11-12), 3339-3362.
846 Volodin, E. M. (2008), Relation between temperature sensitivity to doubled carbon
847 dioxide and the distribution of clouds in current climate models, *Izvestiya, Atmospheric
848 and Oceanic Physics*, 44(3), 288-299.
849 Webb, M. J., F. Lambert, and J. M. Gregory (2013), Origins of differences in climate
850 sensitivity, forcing and feedback in climate models, *Climate Dynamics*, 40(3-4), 677-707.
851 Webb, M. J., et al. (2006), On the contribution of local feedback mechanisms to the range
852 of climate sensitivity in two GCM ensembles, *Climate Dynamics*, 27(1), 17-38.
853 Winker, D. M., M. A. Vaughan, A. Omar, Y. Hu, K. A. Powell, Z. Liu, W. H. Hunt, and
854 S. A. Young (2009), Overview of the CALIPSO mission and CALIOP data processing
855 algorithms, *Journal of Atmospheric and Oceanic Technology*, 26(11), 2310-2323.
856 Wood, R., and C. S. Bretherton (2006), On the relationship between stratiform low cloud
857 cover and lower-tropospheric stability, *Journal of Climate*, 19(24), 6425-6432.
858 Zelinka, M. D., S. A. Klein, and D. L. Hartmann (2012), Computing and Partitioning
859 Cloud Feedbacks Using Cloud Property Histograms. Part II: Attribution to Changes in
860 Cloud Amount, Altitude, and Optical Depth, *Journal of Climate*, 25(11), 3736-3754.
861 Zelinka, M. D., C. Zhou, and S. A. Klein (2016), Insights from a refined decomposition
862 of cloud feedbacks, *Geophys. Res. Lett.*, 43(17), 9259-9269.
863 Zelinka, M. D., S. A. Klein, K. E. Taylor, T. Andrews, M. J. Webb, J. M. Gregory, and P.
864 M. Forster (2013), Contributions of Different Cloud Types to Feedbacks and Rapid
865 Adjustments in CMIP5*, *Journal of Climate*, 26(14), 5007-5027.
866